

Vapor–Liquid Equilibrium Data for the Azeotropic Difluoromethane + Propane System at Temperatures from 294.83 to 343.26 K and Pressures up to 5.4 MPa

Christophe Coquelet, Albert Chareton, Alain Valtz, Abdelatif Baba-Ahmed, and Dominique Richon*

Centre d'Energétique, Ecole Nationale Supérieure des Mines de Paris CENERG/TEP, 35 Rue Saint Honoré, 77305 Fontainebleau, France

Isothermal vapor–liquid equilibrium data for the difluoromethane (R32) + propane binary system are presented at (278.10, 294.83, 303.23, 313.26, and 343.26) K and pressures up to 5.4 MPa. The experimental method is the static–analytic type. It takes advantage of mobile pneumatic capillary samplers (Rolsi, Armines' patent) developed in this laboratory. At a fixed temperature, the azeotrope vapor pressure is larger than those of the pure component. The R32 + propane azeotropic binary system presents two critical points in a specific temperature range. This behavior was verified and visually observed in two supplementary experiments with equipment based on the static–synthetic method involving a variable volume cell. Data along the five isotherms have been represented with the Soave–Redlich–Kwong (SRK) equation of state and MHV1 mixing rules involving the NRTL model. We have calculated the location of the azeotrope by using an equality of equation of state attractive parameters of the two phases.

Introduction

In 1987, the modification of the Montreal protocol¹ has prohibited the use and the production of chlorofluorocarbons (CFCs) in industrialized nations. Knowledge of the thermophysical properties of mixtures containing hydrofluorocarbons (HFCs) and hydrocarbons, which are proposed as alternative refrigerants, is of great importance to evaluate the performance of refrigeration cycles and to determine the optimum composition of new working fluids.

Vapor–liquid equilibria are essential to evaluate both the thermodynamics properties and the efficiency for refrigeration systems. This point was stressed during the second IUPAC Workshop (April 9–11, 2001) on refrigerants (Ecole des Mines, Paris, France), where Dr. J. Morley (DuPont Fluoroproducts, Hemel Hempstead, U.K.) addressed the question: "Are we near an industry standard for refrigerant properties?" He discussed the various important worldwide activities that were taking place to determine accurate thermophysical properties of alternative refrigerant working fluids.

A knowledge of vapor–liquid equilibrium (VLE) data for new mixtures allows a choice of mixtures that offer the most suitable thermodynamic properties. The development of models for representation and prediction of physical properties and phase equilibria as well as the improvement of current equations of state cannot be handled seriously without accurate VLE data.

Using an apparatus based on a static–analytic method, isothermal vapor–liquid equilibrium measurements excluding saturated phase densities on the difluoromethane (R32) + propane binary mixture were performed at temperatures from (278.10 to 343.26) K. The measurements were fitted with the Soave–Redlich–Kwong (SRK) equation of state.

* Corresponding author. E-mail: richon@paris.ensmp.fr. Telephone: 33 164694965. Fax: 33 164694968.

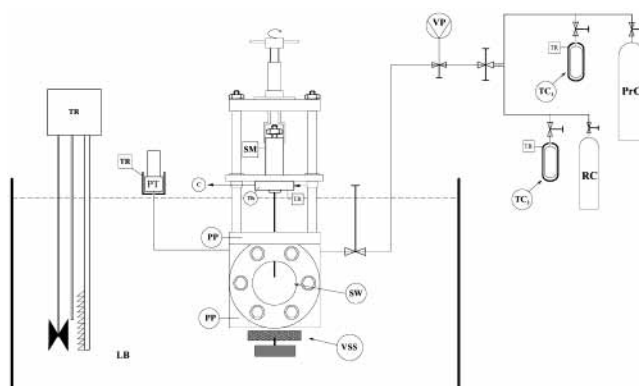


Figure 1. Flow diagram of the equipment: C, carrier gas; EC, equilibrium cell; FV, feeding valve; LB, liquid bath; PP, platinum probe; PrC, propane cylinder; PT, pressure transducer; RC, refrigerant cylinder; SM, sampler monitoring; SW, sapphire window; TC₁ and TC₂, thermal compressors; Th, thermocouple; TR, temperature regulator; VSS, variable speed stirring; VP, vacuum pump.

Experimental Section

Materials. Propane is from Messer Griesheim with a certified purity higher than 99.95 vol %. The difluoromethane (R32) was purchased from DEHON (France) with a certified purity higher than 99.99 vol %. Chemicals were used after degassing the fluids to avoid the presence of incondensable gases.

Apparatus and Experimental Procedures. Most of data have been determined using an apparatus (Figure 1) based on a static–analytic method with liquid and vapor phase sampling. This apparatus is similar to that described by Laugier and Richon.² Remaining data have been determined using a variable volume cell described by Fontalba et al.³ and Valtz et al.⁴

The equilibrium cell is immersed in a thermoregulated liquid bath; the temperature is controlled within 0.01 K.

For accurate temperature measurements in the equilibrium cell and to check for thermal gradients, two platinum resistance thermometers (Pt100) are inserted inside wells drilled into the body of the equilibrium cell at two different levels (see Figure 1) and connected to an HP data acquisition unit (HP34970A). These two Pt100's are periodically calibrated against a 25 Ω reference platinum resistance thermometer (TINSLEY Precision Instruments). The resulting uncertainty is not higher than 0.02 K. The 25 Ω reference platinum resistance thermometer was calibrated by the Laboratoire National d'Essais (Paris) based on the 1990 International Temperature Scale (ITS-90). Pressures are measured by means of a pressure transducer (Druck; type PTX611; range, (0 to 6) MPa) connected to the HP data acquisition unit (HP34970A), as are the two Pt100's; the pressure transducer is maintained at constant temperature (temperature higher than the highest temperature of the study) with a homemade air-thermostat thermally controlled by a PID regulator (WEST instrument, model 6100).

The pressure uncertainty is estimated to be ± 0.001 MPa, after a careful calibration against a dead weight balance (Desgranges & Huot 5202S, CP 0.3 to 40 MPa, Aubervilliers, France).

The HP on-line data acquisition unit is connected to a personal computer through an RS-232 interface. This complete data acquisition system allows real time readings and storage of both temperatures and pressures during isothermal runs.

The analytical work was carried out using a gas chromatograph (VARIAN model CP-3800) equipped with a thermal conductivity detector (TCD). Peak integrations are done on a computer containing a special card from Borwin through the software developed by Borwin (BORWIN ver 1.5, from JMBS, Le Fontanil, France). The analytical column is a HaySep T 100/120 mesh (silcosteel tube; length, 1.6 m; diameter, $\frac{1}{8}$ in.; from Restek). The TCD was repeatedly calibrated by introducing known amounts of each pure compound through a syringe in the injector of the gas chromatograph. Taking into account the uncertainties due to calibrations and dispersions of analyses, the accuracy for vapor and liquid mole fractions is estimated to be 1.0% over the whole range of concentrations.

The experimental procedure is the following: At room temperature, the equilibrium cell and loading circuit were evacuated down to 0.1 Pa. One of the thermal compressors (TC₁) was loaded with R32 while the other (TC₂) was loaded with propane. The required equilibrium temperature was assumed to be reached when the two Pt100 thermometers give the same temperature value within their temperature uncertainty for at least 10 min. Then a volume of about 5 cm³ of propane was introduced into the equilibrium cell. The vapor pressure of propane (the higher boiling temperature component) was recorded at this temperature. To describe the two-phase envelope with at least 10 PT_{xy} data points, adequate amounts of the light component (R32) were introduced step by step, leading to successive new equilibrium mixtures. Equilibrium was assumed when the total pressure remained unchanged within ± 1.0 kPa during a period of 10 min under efficient stirring.

For each equilibrium condition, at least six samples of both vapor and liquid phases were withdrawn using the pneumatic samplers ROLSI as described by Guilbot et al.⁵ and analyzed in order to check for measurement repeatability ($\pm 1\%$).

Table 1. Critical Parameters and Acentric Factors from REFPROP³

compound	P_C /MPa	T_C /K	ω
propane	4.246	369.95	0.152
R32	5.830	351.55	0.271

Correlations

Isothermal VLE measurements on the R32–C₃H₈ system were performed in the temperature range from (278.1 to 343.26) K and at pressures up to 5.4 MPa. The critical temperature (T_C), critical pressure (P_C), and acentric factor (ω), for each pure component are given in Table 1 and are from REFPROP.⁶ Our experimental VLE data are correlated by means of homemade software, THERMOPACK.⁷ The original Soave–Redlich–Kwong⁸ equation of state (SRK EoS) gives good results for VLE of either nonpolar or slightly polar mixtures. It is worthy to note that R32 is a polar compound and the use of the Soave α function would result in systematic deviations between experimental and calculated vapor pressures. We have used the SRK EoS but with the Mathias–Copeman⁹ α function with three adjustable parameters, which was especially developed for polar compounds, given by

$$\alpha(T) = \left[1 + c_1 \left(1 - \sqrt{\frac{T}{T_C}} \right) + c_2 \left(1 - \sqrt{\frac{T}{T_C}} \right)^2 + c_3 \left(1 - \sqrt{\frac{T}{T_C}} \right)^3 \right]^2 \quad (1)$$

where c_1 , c_2 , and c_3 are adjustable parameters. Mathias–Copeman coefficients are evaluated in our whole temperature range using a modified Simplex algorithm. The objective function is

$$F = \frac{100}{N} \sum \left(\frac{P_{\text{exp}} - P_{\text{cal}}}{P_{\text{exp}}} \right)^2 \quad (2)$$

where N is the number of data points, P_{exp} is the measured pressure, and P_{cal} is the calculated pressure.

In our equation of state approach, we need a mixing rule and an activity coefficient model. For these purposes we have selected the MHV1 (modified Huron–Vidal) mixing rule proposed by Michelsen,¹⁰ where the attractive parameter is calculated from eq 3 and the molar covolume from eq 4

$$a = b \left[\sum_i x_i \frac{a_i}{b_i} - \frac{RT}{q_1} \sum_i x_i \ln \left(\frac{b_i}{b} \right) + \frac{G_v^E(T, P, x_j)}{q_1} \right] \quad (3)$$

$$b = \sum_i x_i b_i \quad (4)$$

The reference pressure is $P = 0$. Michelsen recommends $q_1 = -0.593$.

The excess Gibbs energy is calculated using the NRTL¹¹ local composition model,

$$\frac{G_{(T,P)}^E}{RT} = \sum_i x_i \sum_j \frac{x_j \exp \left(-\alpha_{j,i} \frac{\tau_{j,i}}{RT} \right)}{\sum_k x_k \exp \left(-\alpha_{k,i} \frac{\tau_{k,i}}{RT} \right)} \tau_{j,i} \quad (5)$$

where $\tau_{i,i} = 0$ and $\alpha_{i,i} = 0$, and $\alpha_{j,i}$, $\tau_{j,i}$, and $\tau_{i,j}$ are adjustable parameters. For our system which belongs to a given polar

Table 2. Adjusted Mathias–Copeman Coefficients

coefficients	R32	propane
C_1	1.034	0.789
C_2	-1.454	-0.894
C_3	4.038	2.716

Table 3. Experimental and Calculated Vapor Pressures of R32 (SRK EoS)

T/K	$P_{\text{exp}}/\text{MPa}$	$P_{\text{cal}}/\text{MPa}$	$\Delta P/\text{MPa}$
283.19	1.111	1.108	0.003
288.21	1.286	1.282	0.004
293.24	1.481	1.477	0.004
298.26	1.697	1.692	0.005
303.27	1.935	1.931	0.004
308.28	2.197	2.194	0.003
313.30	2.485	2.485	0.000
318.28	2.801	2.802	0.001
323.30	3.147	3.153	-0.006
328.31	3.526	3.536	-0.010
343.26	4.892	4.905	0.013

Table 4. Experimental and Calculated Vapor Pressures of Propane (SRK EoS)

T/K	$P_{\text{exp}}/\text{MPa}$	$P_{\text{cal}}/\text{MPa}$	$\Delta P/\text{MPa}$
277.17	0.536	0.535	0.001
283.22	0.638	0.638	0.000
288.26	0.734	0.734	0.000
293.27	0.838	0.839	0.001
298.30	0.955	0.955	0.000
302.27	1.055	1.055	0.000
308.80	1.236	1.236	0.000
311.80	1.326	1.326	0.000
313.24	1.370	1.371	-0.001
318.22	1.537	1.536	0.001
323.22	1.716	1.715	0.001
328.26	1.911	1.911	0.000
333.29	2.120	2.122	-0.002
338.31	2.346	2.350	-0.004
343.26	2.591	2.593	-0.002
348.31	2.852	2.859	-0.007
353.41	3.134	3.149	-0.014

mixture type it is recommended¹¹ to use $\alpha_{ji} = 0.3$. The τ_{ji} and τ_{ij} are adjusted directly to VLE data through a modified Simplex algorithm using the objective function

$$F = \frac{100}{N} \left[\sum \left(\frac{P_{\text{exp}} - P_{\text{cal}}}{P_{\text{exp}}} \right)^2 \right] \quad (6)$$

Results and Discussion

Vapor Pressures. Two vapor pressure correlations were used to generate enough data in order to fit the Mathias–Copeman coefficients: Tillner–Roth's¹² correlation for R32 and the McLinden's¹³ correlation for propane, from 248 K to the critical temperatures of the corresponding component. The calculated values of the SRK EoS Mathias–Copeman coefficients are reported in Table 2. We have also measured the vapor pressures of the two pure components. Tables 3 and 4 (R32 and propane, respectively) report both our experimental data and pressures calculated with our model using the determined Mathias–Copeman coefficients. We have good agreement between experimental and calculated vapor pressures, showing good consistency between experimental data, literature correlations, and our data treatment through the RKS EoS + Mathias–Copeman α function. The α functions are valid between 248 K and the critical temperatures of the considered components.

Vapor–Liquid Equilibrium. The VLE data obtained are listed in Tables 5–10. At each temperature, we have adjusted the two (τ_{ji} and τ_{ij}) NRTL parameters. They

Table 5. Vapor–Liquid Equilibrium Pressures and Phase Compositions for R32 (1) + Propane (2) Mixtures at 278.10 K

experimental data			calculated data			
$P_{\text{exp}}/\text{MPa}$	x_1	$y_{1\text{exp}}$	$P_{\text{cal}}/\text{MPa}$	$y_{1\text{cal}}$	$\Delta P/\text{MPa}$	Δy
0.553	0.000	0.000	0.550	0.000	-0.003	0.000
0.727	0.043	0.236	0.726	0.243	-0.001	-0.007
0.936	0.124	0.419	0.944	0.431	0.008	-0.012
1.109	0.262	0.526	1.121	0.544	0.012	-0.018
1.189	0.424	0.596	1.197	0.599	0.008	-0.003
1.201	0.474	0.610	1.208	0.611	0.007	-0.001
1.209	0.516	0.622	1.216	0.620	0.007	0.002
1.215	0.563	0.634	1.222	0.631	0.007	0.003
1.218	0.583	0.639	1.223	0.635	0.005	0.004
1.220	0.608	0.646	1.225	0.641	0.005	0.005
1.221	0.628	0.651	1.226	0.646	0.005	0.005
1.222	0.673	0.664	1.226	0.658	0.004	0.006
1.221	0.680	0.666	1.226	0.660	0.005	0.006
1.214	0.756	0.693	1.217	0.687	0.003	0.006
1.205	0.791	0.711	1.208	0.704	0.003	0.007
1.131	0.909	0.805	1.129	0.801	-0.002	0.004
1.023	0.975	0.921	1.016	0.923	-0.007	-0.002
0.956	1.000	1.000	0.950	1.000	-0.006	0.000

Table 6. Vapor–Liquid Equilibrium Pressures and Phase Compositions for R32 (1) + Propane (2) Mixtures at 294.83 K

experimental data			calculated data			
$P_{\text{exp}}/\text{MPa}$	x_1	$y_{1\text{exp}}$	$P_{\text{cal}}/\text{MPa}$	$y_{1\text{cal}}$	$\Delta P/\text{MPa}$	Δy
0.874	0.000	0.000	0.874	0.000	0.000	0.000
0.926	0.008	0.049	0.922	0.050	-0.004	-0.001
1.123	0.046	0.206	1.121	0.216	-0.002	-0.010
1.206	0.064	0.261	1.202	0.269	-0.004	-0.008
1.406	0.123	0.370	1.413	0.385	0.007	-0.015
1.693	0.264	0.508	1.699	0.511	0.006	-0.003
1.840	0.439	0.584	1.851	0.586	0.011	-0.002
1.897	0.599	0.645	1.908	0.641	0.011	0.004
1.900	0.618	0.650	1.911	0.648	0.011	0.002
1.906	0.694	0.684	1.913	0.678	0.007	0.006
1.903	0.731	0.699	1.908	0.695	0.005	0.004
1.897	0.759	0.713	1.900	0.709	0.003	0.004
1.880	0.802	0.746	1.881	0.735	0.001	0.011
1.715	0.941	0.877	1.710	0.875	-0.005	0.002
1.677	0.957	0.903	1.672	0.903	-0.005	0.000
1.547	1.000	1.000	1.542	1.000	-0.005	0.000

Table 7. Vapor–Liquid Equilibrium Pressures and Phase Compositions for R32 (1) + Propane (2) Mixtures at 303.23 K

experimental data			calculated data			
$P_{\text{exp}}/\text{MPa}$	x_1	$y_{1\text{exp}}$	$P_{\text{cal}}/\text{MPa}$	$y_{1\text{cal}}$	$\Delta P/\text{MPa}$	Δy
1.255	0.027	0.126	1.253	0.130	-0.002	-0.004
1.492	0.073	0.258	1.495	0.270	0.003	-0.012
1.824	0.165	0.404	1.833	0.413	0.009	-0.009
2.076	0.287	0.503	2.090	0.506	0.014	-0.003
2.262	0.456	0.590	2.272	0.583	0.010	0.007
2.311	0.535	0.615	2.320	0.615	0.009	0.000
2.317	0.564	0.630	2.332	0.626	0.015	0.004
2.336	0.646	0.665	2.352	0.661	0.016	0.004
2.340	0.694	0.689	2.353	0.684	0.013	0.005
2.345	0.705	0.695	2.352	0.689	0.007	0.006
2.318	0.794	0.747	2.320	0.740	0.002	0.007
2.226	0.890	0.824	2.218	0.821	-0.008	0.003
2.094	0.953	0.916	2.084	0.905	-0.010	0.011
1.937	1.000	1.000	1.929	1.000	-0.008	0.000

appear slightly temperature dependent, as shown in Figures 2 and 3.

Second-order relationships are adequate for their representation, as given by

$$\tau_{12} = 0.215 T^2 - 133.44 T + 23579.72 \quad (7)$$

$$\tau_{21} = -0.139 T^2 + 77.35 T - 8387.20 \quad (8)$$

Table 8. Vapor–Liquid Equilibrium Pressures and Phase Compositions for R32 (1) + Propane (2) Mixtures at 313.26 K

experimental data			calculated data			
$P_{\text{exp}}/\text{MPa}$	x_1	$y_{1\text{exp}}$	$P_{\text{cal}}/\text{MPa}$	$y_{1\text{cal}}$	$\Delta P/\text{MPa}$	Δy
1.496	0.017	0.075	1.497	0.077	0.001	-0.002
1.608	0.034	0.133	1.613	0.138	0.005	-0.005
2.344	0.198	0.412	2.363	0.417	0.019	-0.005
2.540	0.272	0.475	2.555	0.472	0.015	0.003
2.720	0.367	0.530	2.730	0.526	0.010	0.004
2.844	0.468	0.583	2.859	0.575	0.015	0.008
2.931	0.582	0.639	2.949	0.631	0.018	0.008
2.940	0.605	0.649	2.960	0.642	0.020	0.007
2.952	0.622	0.658	2.966	0.651	0.014	0.007
2.964	0.710	0.705	2.975	0.699	0.011	0.006
2.923	0.799	0.761	2.934	0.756	0.011	0.005
2.880	0.844	0.797	2.887	0.792	0.007	0.005
2.685	0.947	0.901	2.677	0.906	-0.008	-0.005
2.491	1.000	1.000	2.483	1.000	-0.008	0.000

Table 9. Vapor–Liquid Equilibrium Pressures and Phase Compositions for R32 (1) + Propane (2) Mixtures at 343.26 K

experimental data			calculated data			
$P_{\text{exp}}/\text{MPa}$	x_1	$y_{1\text{exp}}$	$P_{\text{cal}}/\text{MPa}$	$y_{1\text{cal}}$	$\Delta P/\text{MPa}$	Δy
2.591	0.000	0.000	2.593	0.000	0.002	0.000
3.139	0.065	0.146	3.165	0.148	0.026	-0.002
3.499	0.113	0.226	3.519	0.220	0.020	0.006
3.964	0.188	0.310	3.977	0.297	0.013	0.013
4.222	0.237	0.345	4.225	0.333	0.003	0.012
4.442	0.282	0.375	4.423	0.360	-0.019	0.015
4.702	0.345	0.420	4.658	0.388	-0.044	0.032
5.009	0.432	0.472	5.003	0.432	-0.006	0.040
5.077	0.457	0.480	5.075	0.457	-0.002	0.023
5.451	0.858	0.849	5.451	0.858	0.000	-0.009
5.413	0.876	0.866	5.415	0.873	0.002	-0.007
5.308	0.911	0.901	5.313	0.900	0.005	0.001
5.259	0.924	0.915	5.267	0.912	0.008	0.003
5.201	0.939	0.930	5.208	0.927	0.007	0.003
5.049	0.972	0.965	5.058	0.964	0.009	0.001
4.940	0.992	0.989	4.951	0.989	0.011	0.000
4.892	1.000	1.000	4.905	1.000	0.013	0.000

Table 10. Mean Relative Absolute Deviations in Pressure, MRDP, Vapor Phase Compositions, MRDY, and Bias Using the Soave–Redlich–Kwong Equation of State with MHV1 Mixing Rules

T/K	$\text{bias}(P)/\%$	$\text{MRD}(P)/\%$	$\text{bias}(y)/\%$	$\text{MRD}(y)/\%$
278.10	0.25	0.50	-0.18	0.96
294.83	0.10	0.33	-0.59	1.18
303.23	0.22	0.43	-0.32	1.24
313.26	0.14	0.26	0.02	1.15
343.26	0.09	0.26	1.93	2.31

The results of modeling are reported in Tables 5–9 and plotted in Figure 4.

The mean relative absolute percentage deviations on pressure, $\text{MRD}(P)$, and the mean relative percentage deviations on vapor phase mole fraction, $\text{MRD}(y)$, listed in Table 10, are defined by

$$\text{MRD}(U) = (100/N) \sum [(U_{\text{cal}} - U_{\text{exp}})/U_{\text{exp}}] \quad (9)$$

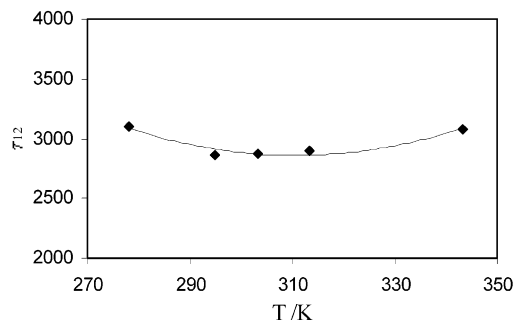
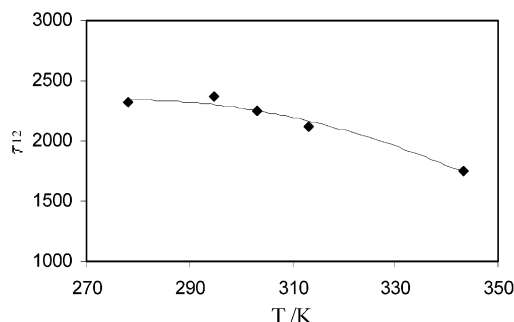
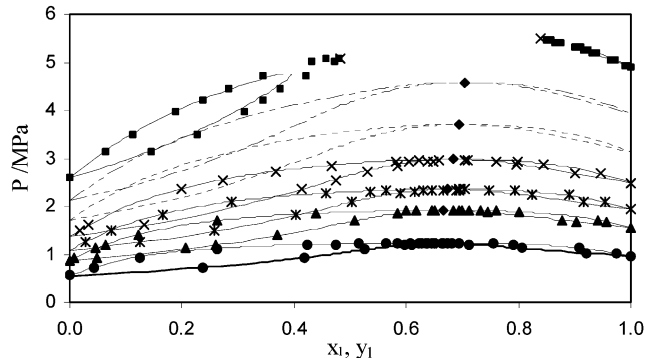
where $U = P$ or y_1 and N is the number of data points.

We have also calculated the bias values which are listed in Table 10 and defined by eq 10:

$$\text{bias}(U) = (100/N) \sum ((U_{\text{exp}} - U_{\text{cal}})/U_{\text{exp}}) \quad (10)$$

where $U = P$ or y_1 and N is the number of data points.

An accurate representation of the experimental data is found except at 343.26 K, where adjustment and modeling

**Figure 2.** τ_{12} NRTL binary parameter as a function of temperature: \blacklozenge , fitted to isotherm; —, eq 7.**Figure 3.** τ_{21} NRTL binary parameter as a function of temperature: \blacklozenge , fitted to isotherm; —, eq 8.**Figure 4.** VLE for the R32 (1) + propane (2) system at different temperatures: \bullet , 278.10 K; \blacktriangle , 294.83 K; $*$, 303.23 K; \times , 313.26 K; \blacksquare , 343.26 K; +, graphical end points; solid lines, calculated with RKS EoS and MHV1 mixing rules; ---, calculated at 323 K; - · -, calculated at 333 K; \blacklozenge , azeotrope location.

are very difficult. At the mixture critical point the equation of state must calculate identical molar volumes for liquid and vapor phases. However, the SRK cubic equation of state is unable to calculate high-accuracy molar volumes close to the critical region. This may be the main reason for the modeling difficulty here.

PVT Method. We have used another method to get results, especially in the region where two critical points appear and a poor representation was obtained. This method (a static–synthetic one with a variable volume cell) was used to verify the data obtained from the static–analytic method. Herein, we measured only bubble pressures and compared them against the correlations. The uncertainties are within ± 0.004 MPa for the pressures and ± 0.1 K for the temperatures. As displayed in Table 11, there is a good agreement (less than 1% for relative pressure deviation) between the two experimental methods. We have shown that left-hand part of the diphasic envelope at 343.26 K really extends to x_{R32} about 0.5 while modeling stops at about 0.4. At this temperature there is clearly a modeling problem, not an experimental one. So we have

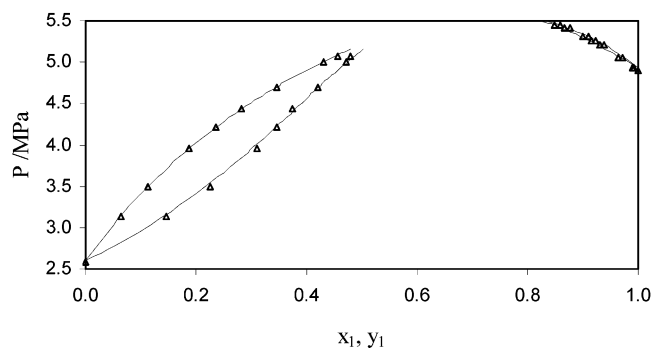


Figure 5. VLE for the R32 (1) + propane (2) system at 343.26 K: solid lines, calculated with PR EoS and Wong-Sandler mixing rules.

Table 11. Bubble Point Data Measured by the PVT Method and Calculated by SRK + MHV1 + NRTL Models (R32 (1) + Propane (2) Mixtures)

T/K	$P_{\text{exp}}/\text{MPa}$	x_1	$P_{\text{cal}}/\text{MPa}$	$y_{1\text{cal}}$	$\Delta P/\text{MPa}$
287.53	1.533	0.439	1.542	0.593	-0.009
295.38	1.869	0.465	1.890	0.594	-0.021
303.67	2.278	0.465	2.302	0.586	-0.024
313.02	2.817	0.465	2.841	0.574	-0.024
323.16	3.572	0.866	3.570	0.824	0.002
323.25	3.455	0.439	3.482	0.542	-0.027
323.35	3.497	0.465	3.532	0.556	-0.035
332.75	4.404	0.866	4.391	0.838	0.013
333.04	4.186	0.439	4.207	0.509	-0.021
333.17	4.251	0.465	4.278	0.524	-0.027
333.49	4.090	0.388	4.109	0.477	-0.019
333.49	4.129	0.406	4.156	0.487	-0.027
337.85	4.629	0.465	4.641	0.493	-0.012
340.42	4.739	0.465	4.698	0.465	0.041
342.15	4.874	0.406	4.823	0.406	0.051
343.10	3.876	0.173	3.884	0.284	-0.008
343.18	4.821	0.388	4.780	0.388	0.041

changed the EoS and the mixing rules in order to have the best densities calculation.

The Peng Robinson¹⁴ equation of state associated with the Wong-Sandler¹⁵ mixing rules represents very well the 343.26 K isotherm. The Wong-Sandler mixing rules are much more flexible than the MHV1 rules with their third k_{ij} parameter. As a consequence, all the densities are better calculated and the experimental data are better represented, especially at high pressures. The value of each parameter is given below, and the 343.26 K isotherm is plotted in Figure 5.

$$\tau_{12} = 1317, \quad \tau_{21} = 3135, \quad k_{12} = 0.359$$

Azeotrope Line Computation. An azeotrope corresponds to an extremum of temperature or pressure. At this point the compositions of both liquid and vapor phases are equal. This can be expressed by

$$\left(\frac{\partial T}{\partial x_i}\right)_P = 0 \quad \text{for } i = 1 \text{ to } N-1 \quad (11)$$

$$\left(\frac{\partial P}{\partial x_i}\right)_T = 0 \quad \text{for } i = 1 \text{ to } N-1 \quad (12)$$

$$x_i = y_i \quad \text{for } i = 1 \text{ to } N \quad (13)$$

An azeotrope behaves like a pure fluid and then its components cannot be separated by simple distillation. Consequently, at equilibrium, EoS mixtures attractive parameters (a) for the azeotrope composition are the same in both the liquid and the vapor phases. Satisfying this

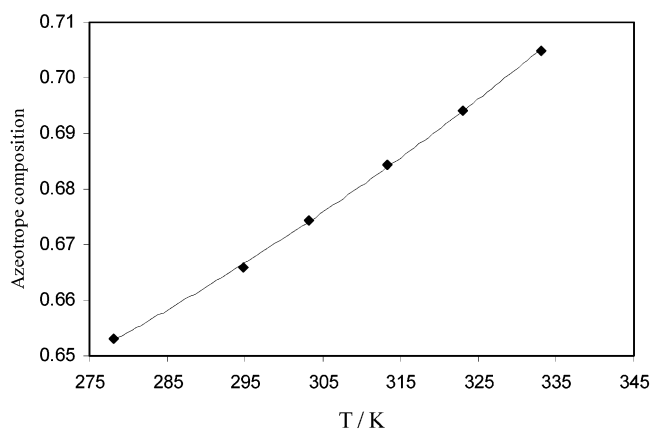


Figure 6. Azeotropic composition (R32) as function of temperature: \blacklozenge , calculated azeotrope; \bullet , eq 14.

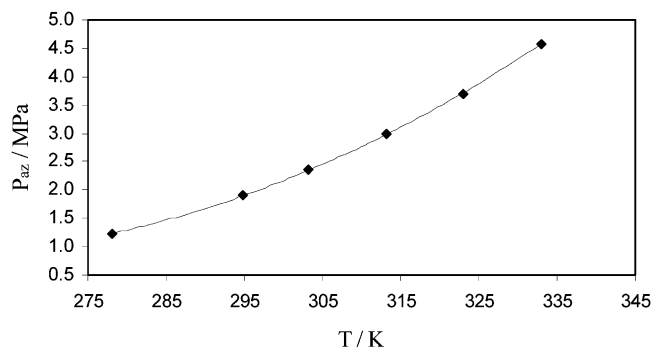


Figure 7. Azeotropic pressure as function of temperature: \blacklozenge , calculated azeotrope; \bullet , eq 15

Table 12. Composition and Pressure of the Azeotrope (R32) at Each Temperature (MHV1 Mixing Rules)

T/K	$x_{\text{az,exp}}$	$P_{\text{exp}}/\text{MPa}$	$x_{\text{az,cal}}$	$P_{\text{cal}}/\text{MPa}$	$\Delta P/\text{MPa}$	Δx
278.10	0.663	1.221	0.653	1.226	-0.005	0.010
294.83	0.679	1.906	0.666	1.914	-0.008	0.023
303.23	0.683	2.342	0.674	2.354	-0.012	0.009
313.26	0.702	2.961	0.684	2.977	-0.016	0.018
323.00			0.694	3.699		
333.00			0.705	4.580		

equality condition allows us to compute the azeotrope location. This method is suitable with an equation of state for either isothermal or isobaric calculations.

Analytically, the advantage of this method is there are no derivatives to calculate. A simple secant method permits us to obtain $a^l = a^v$ at equilibrium, where the compositions of the two phases are equal ($x_i = y_i$).

The computational algorithm is as follows: (i) input composition; (ii) calculate $a^v - a^l$ at equilibrium; (iii) search for another composition where $\prod_i (a^v - a^l)_i < 0$ at equilibrium; and (iv) use the secant method to obtain the composition where $a^v - a^l = 0$.

We show in Table 12 and Figures 6 and 7 the characteristics of the azeotrope (pressure, temperature, and composition). Equations 14 and 15 give the relation between T , P_{az} , and x_{az} (R32).

$$P_{\text{az}} = 379.61x_{\text{az}}^2 - 451.39x_{\text{az}} + 134.13 \quad (14)$$

$$P_{\text{az}} = (5.498 \times 10^{-4})T^2 - 0.275T + 35.26 \quad (15)$$

Note that the azeotropic composition of R32 increases with temperature.

Comparison with Literature Data. Bobbo et al.¹⁶ obtained data for this system at lower temperatures but

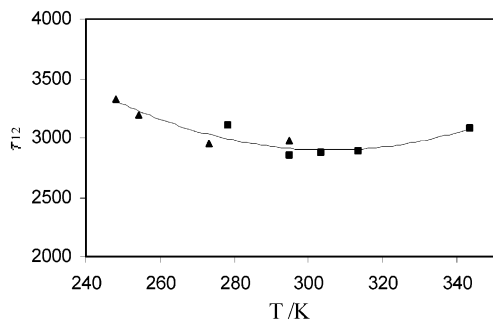


Figure 8. τ_{12} NRTL binary parameter as function of temperature: \blacktriangle , from Bobbo et al.; \blacksquare , this work; —, eq 16.

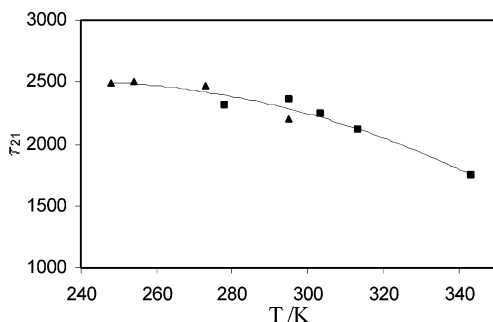


Figure 9. τ_{21} NRTL binary parameter as function of temperature: \blacktriangle , from Bobbo et al.; \blacksquare , this work; —, eq 17.

Table 13. Mean Relative Absolute Deviations in Pressure, MRD(P), Vapor Phase Composition, MRD(y), and Bias Using the Soave–Redlich–Kwong Equation of State with MHV1 Mixing Rules

ref	T/K	bias(P)/%	MRD(P)/%	bias(y)/%	MRD(y)/%
16	248.15	-0.18	0.26	0.46	0.63
	254.15	-0.11	0.45	-0.03	0.74
	273.15	-0.05	0.41	1.20	1.21
	294.91	-0.08	0.36	0.96	1.05
this work	278.10	0.39	0.42	-0.09	0.74
	294.83	0.37	0.38	-0.25	0.79
	303.23	0.27	0.33	0.03	0.19
	313.26	0.12	0.16	0.29	0.75
	343.26	0.12	0.25	2.60	2.91

did not reproduce the liquid–liquid equilibrium mentioned by Holcomb et al.¹⁶ We have fitted our model to their data. Then, we obtained two new parameters at each of their temperatures. Equations 16 and 17 represent the temperature dependence of the parameters obtained for each of our and Bobbo et al.'s temperatures, (248.15 to 343.26) K. The temperature dependence of the parameters is continuous (see Figures 8 and 9), indicating consistency between the two data sets.

$$\tau_{12} = 0.189T^2 - 111.73T + 19375 \quad (16)$$

$$\tau_{21} = -0.098T^2 + 49.78T - 3817 \quad (17)$$

The BIAS(U) and MRD(U) were also calculated, and the results are reported in Table 13. There is good agreement between experimental data and calculated data using the parameters τ_{12} and τ_{21} (eqs 16 and 17). Figure 10 gives the predictive curves along with experimental data (the 343.26 K isotherm does not appear in this figure).

Supercritical State. At 343.26 K, we have pointed out the disappearance of the phase separation for x_{R32} between 0.5 and 0.85. The mixture becomes supercritical although the equilibrium temperature is lower than the critical

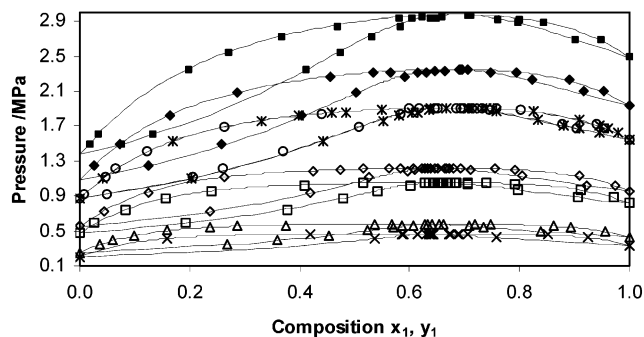


Figure 10. VLE for the R32 (1) + propane (2) system at all different temperatures with experimental data.

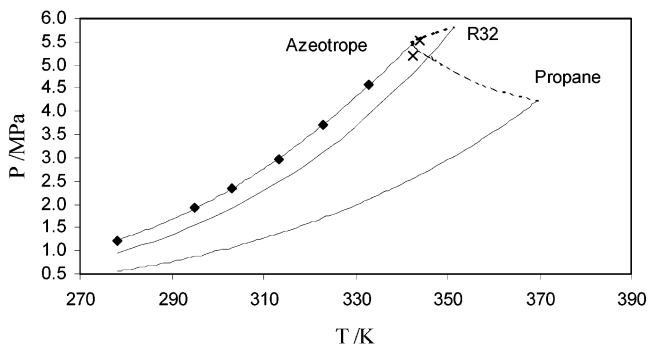


Figure 11. PT diagram of the R32 + propane system: ---, critical locus from Van Poolen et al.; \times , critical point measured by the PVT (sapphire cell); \blacklozenge , azeotrope calculation.

Table 14. Critical Points Measured by the PVT Equipment with a Sapphire Variable Volume Cell

T/K	P/MPa	x_{R32}
342.50	5.210	0.527
344.00	5.532	0.866

temperature of the lightest component (R32). This isotherm and its two graphical critical end points are shown in Figure 4. An apparatus using the sapphire cell described by Laugier et al.¹⁸ was used to observe the phase transition. At the critical point, a fog can be observed when the pressure is decreased. With this technique, we can record the pressure and the temperature for one composition after several cycles of increasing and decreasing of temperature. Two bubble pressures were measured, and the results are given in Table 14. The precision for the pressure is ± 0.004 MPa, and it is ± 0.1 K for the temperature. A correlating method to represent the critical point locus was established by Van Poolen et al.¹⁹ Our critical data are congruent with the correlation. Figure 11 shows a plot indicating the VLE domain including the azeotrope and the critical lines from Van Poolen et al.¹⁹

Conclusion

In this paper, we present VLE data for the propane + R32 system along several isotherms. Two experimental methods were used to verify the behavior of this system. A static–analytic method and a PVT method were used to obtain the experimental data. The Soave–Redlich–Kwong equation of state (SRK EoS), with a Mathias–Copeman α function and MHV1 mixing rules, was chosen to fit VLE data, except for the 343.26 K isotherm, where the Peng–Robinson (PR) and the Wong–Sandler mixing rules were used. At this temperature, there are two critical points. The azeotrope location is given as a function of temperature (see Figure 11).

List of Symbols

a = parameter of the equation of state (attractive parameter)
 b = parameter of the equation of state (covolume parameter)
 G = Gibbs free energy
 F = objective function
 P = pressure
 R = gas constant
 T = temperature
 Z = compressibility factor
 x = liquid mole fraction
 y = vapor mole fraction
 N = number of components

Greek Letters

α_{ij} = NRTL model parameter (eq 5)
 τ_{ij} = NRTL model binary interaction parameter (eq 5)
 ω = acentric factor
 Δ = deviation

Superscript

E = excess property

Subscripts

C = critical property
cal = calculated property
exp = experimental property
 i, j = molecular species
az = azeotrope
v = vapor phase
l = liquid phase
1 = R32
2 = propane

Literature Cited

- (1) Montreal Protocol on substances that deplete the ozone layer, United Nations Environmental Program (UNEP), Final Act, United Nations, New York, USA, 1987.
- (2) Laugier, S.; Richon, D. New apparatus to perform fast determinations of mixture vapor – liquid equilibria up to 10 MPa and 423 K. *Rev. Sci. Instrum.* **1986**, *57*, 469–472.

- (3) Fontalba, F.; Richon, D.; Renon, H. Simultaneous determination of PVT and VLE data of binary mixtures up to 45 MPa and 433 K: a new apparatus without phase sampling and analysis. *Rev. Sci. Instrum.*, **1984**, *55* (6), 944–951.
- (4) Valtz, A.; Laugier, S.; Richon, D. Bubble pressures and saturated liquid molar volumes of difluoromonochloromethane-fluorochloroethane binary mixtures: experimental data and modeling. *Int. J. Refrig.* **1986**, *9*, 282–289.
- (5) Guilbot, P.; Valtz, A.; Legendre, H.; Richon, D. Rapid On Line Sampler-Injector, a reliable tool for HT-HP Sampling and on line GC analysis. *Analisis* **2000**, *28*, 426–431.
- (6) Huber, M.; Gallagher, J.; McLinden, M. O.; Morrison, G. *Thermodynamic Properties of Refrigerants and Refrigerant Mixtures Database*, REFPROP V.6.01; National Institute of Standards and Technology: Gaithersburg, MD, 1996.
- (7) 17th IUPAC Conference on Chemicals Thermodynamics, Rostock, July 28 to August 02, 2002.
- (8) Soave, G. Equilibrium constants for modified Redlich-Kwong equation of state. *Chem. Eng. Sci.* **1972**, *4*, 1197–1203.
- (9) Mathias, P. M.; Copeman, T. W. Extension of the Peng–Robinson Equation of State to Complex Mixtures: Evaluation of Various Forms of the Local Composition Concept. *Fluid Phase Equilib.* **1983**, *13*, 91–108.
- (10) Michelsen, M. A modified HURON–VIDAL mixing rule for cubic equations of state. *Fluid Phase Equilib.* **1990**, *60*, 213–219.
- (11) Renon, H.; Prausnitz, J. M. Local Composition in Thermodynamic Excess Function for Liquid Mixtures. *AIChE J.* **1968**, *14*, 135–144.
- (12) Tillner-Roth, R.; Yokozeki, A. An international standard equation of state for difluoromethane (R32) for temperatures from triple point at 136.34 K to 435 K and pressures up to 70 MPa. *J. Phys. Ref. Data* **1997**, *26*, 1273–1328.
- (13) McLinden, M. O. Thermodynamic properties of CFC alternatives: a survey of the available data. *Int. J. Refrig.* **1990**, *13*, 149–162.
- (14) Peng, D. Y.; Robinson, D. B. A new two parameters Equation of State. *Ind. Eng. Chem. Fundam.* **1976**, *15*, 59–64.
- (15) Wong, D. S. H.; Sandler, S. I. A Theoretically Correct Mixing Rules for Cubic Equation of State. *AIChE J.* **1992**, *38*, 671–680.
- (16) Bobbo, S.; Fedele, L.; Camporese, R.; Stryjek, R. VLE measurements and modeling for the strongly positive azeotropic R32 + propane system. *Fluid Phase Equilib.* **2002**, *199*, 175–183.
- (17) Holcomb, C. D.; Magee, J. W.; Scott, J. R.; Outcalt, S. L.; Haynes, W. M. NIST Technical Note 1397; NIST: Gaithersburg, December 1997.
- (18) Laugier, S.; Richon, D.; Renon, H. Simultaneous determination of vapor-liquid equilibria and volumetric properties of ternary systems with a new experimental apparatus. *Fluid Phase Equilib.* **1990**, *54*, 19–34.
- (19) Van Poolen, L. J.; Holcomb, C. D.; Rainwater, J. C. Isoplethic method to Estimate Critical lines for Binary Fluid Mixtures from Subcritical Vapor-Liquid Equilibrium: Application to the Azeotropic Mixtures R32 + C₃H₈ and R125 + C₃H₈. *Ind. Eng. Chem. Res.* **2001**, *40*, 4610–4614.

Received for review June 19, 2002. Accepted December 3, 2002.

JE020115D